Spin-split silicon states at step edges of Si(553)-Au

K. Biedermann, S. Regensburger, Th. Fauster, F. J. Himpsel, and S. C. Erwin

Phys. Rev. B **85**, 245413 — Published 6 June 2012

DOI: 10.1103/PhysRevB.85.245413

Spin-split silicon states at step edges of Si(553)-Au

K. Biedermann, S. Regensburger, and Th. Fauster

Lehrstuhl für Festkörperphysik, Universität Erlangen-Nürnberg,

Staudtstraße 7, 91058 Erlangen, Germany

F. J. Himpsel

Department of Physics, University of Wisconsin-Madison,

1150 University Avenue, Madison, WI 53706, USA

S. C. Erwin

Center for Computational Materials Science,

Naval Research Laboratory, Washington, DC 20375, USA

Abstract

The quasi one-dimensional Si(553)-Au surface is investigated with time-resolved two-photon photoemission and laser-based photoemission. Several occupied and unoccupied states in and outside the bulk band gap of silicon were found near the center of the surface Brillouin zone. A non-dispersing unoccupied state 0.62 eV above the Fermi level with a lifetime of 125 fs matches the spin-split silicon step-edge state predicted by density-functional-theory calculations. Two occupied bands can be associated with the bands calculated for non-polarized step-edge atoms.

PACS numbers: 73.20.At, 79.60.Jv, 82.53.Mj

I. INTRODUCTION

Submonolayers of gold on vicinal Si(111) surfaces form a variety of atomic chain structures that are excellent realizations of one-dimensional electronic model systems.[1] Although the gold atoms are rigidly locked to the substrate, electronic states near the Fermi level E_{F} lie inside the band gap of silicon and thus cannot hybridize with the three-dimensional states of the substrate. These surfaces have been investigated in detail both theoretically[2–7] and experimentally[1,2,8–19] with particular emphasis on the exotic phenomena predicted for one-dimensional electrons.

The most perfect of these vicinal surfaces is Si(553)-Au,[11] which exhibits a miscut angle of 12.5° from the [111] direction towards $[11\overline{2}]$. Its (111) terraces are 1.48 nm wide and contain 2.1 ± 0.4 gold atoms per (553)-1×1 unit cell, running parallel to the single-height atomic steps.[2,19] The latest structural model consists of a gold double chain on each terrace and a silicon honeycomb chain at the step edge.[6,7]

Density-functional-theory (DFT) calculations predict that in the ground state of Si(553)-Au, every third silicon atom at the step edge is fully spin-polarized.[7] The spin-polarized atoms create a ×3 modulation of the electron density along the step edges, which explains the periodic lattice distortions (or charge-density waves) previously observed in scanning tunneling microscopy (STM).[1,9–11] The gold double chain creates two metallic bands strongly dispersing in the direction parallel to the gold chains with minima at the boundary of the 1×1 Brillouin zone, as observed in photoemission. The two gold bands are slightly split by the spin-orbit interaction,[7] and the larger splitting of the lower band has been observed in photoemission.[14] The exchange interaction strongly splits the one of the three silicon step-edge bands.[7] This exchange splitting dramatically shifts the unoccupied minority spin band to ∼0.5 eV above the Fermi level. Because this energy region is devoid of any other narrow bands, the experimental detection of this predicted state should be possible—and would strongly support the predicted spin-polarized ground state.

While the occupied part of the band structure of Si(553)-Au has been investigated in great detail by angle-resolved photoemission spectroscopy,[1,2,8,9,14,15] the unoccupied bands remained largely unexplored. Since the Fermi level of Si(553)-Au is pinned close to the valence band maximum, most occupied surface states overlap with bulk bands near the zone center. Unoccupied states up to $\approx$ 1 eV above the Fermi energy lie in the band gap and

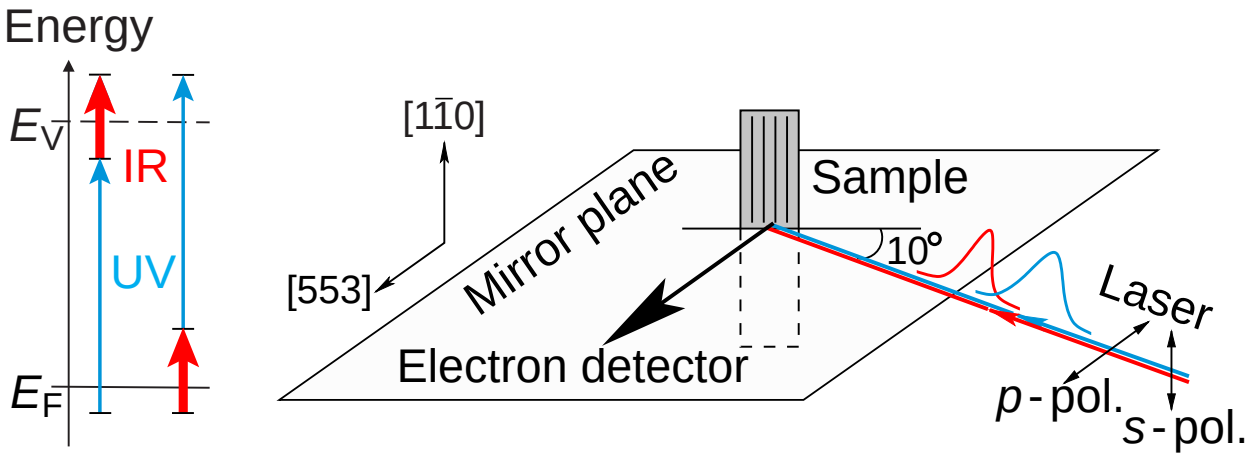

FIG. 1. (Color online) Left: Possible two-photon photoemission processes. Right: Experimental geometry showing a sample with the gold chains and step edges oriented perpendicular to the plane of incidence, i. e. the mirror plane is in the plane of incidence. *In situ* azimuthal rotation of the sample by 90° allows measurement of the dispersion along the step edges.

thus are truly two- or one-dimensional. Experimental studies of these unoccupied surface states have not been reported yet to our knowledge.

In this study we use two-photon photoemission (2PPE) to investigate the energy region between the Fermi level E_F and vacuum level E_V as sketched in the left part of Fig. 1. The combination of infrared (IR) and ultraviolet (UV) photons makes energy ranges of about 1.5 eV below the vacuum level and above the Fermi level accessible, depending on the time sequence of the IR and UV pulses. Additional information about the symmetry of the involved states is obtained from polarization-dependent laser-excited single-photon photoemission (1PPE). These methods have been successfully applied to Si(557)-Au.[20,21]

II. EXPERIMENTAL TECHNIQUES

Si(553)-Au surfaces were prepared on p-type silicon substrates (resistivity $\approx 0.1\ \Omega$cm) in ultrahigh vacuum (base pressure $< 5 \times 10^{-11}$ mbar) following procedures described in detail in the literature.[2,20] The sample preparation was optimized by low-energy electron diffraction (LEED). Figure 2 shows a diffraction pattern with faint half- and third-order horizontal streaks which are characteristic of the (1×2) and (1×3) reconstruction of the gold chains and step-edge atoms, respectively.[7] The steps and chains are oriented vertically

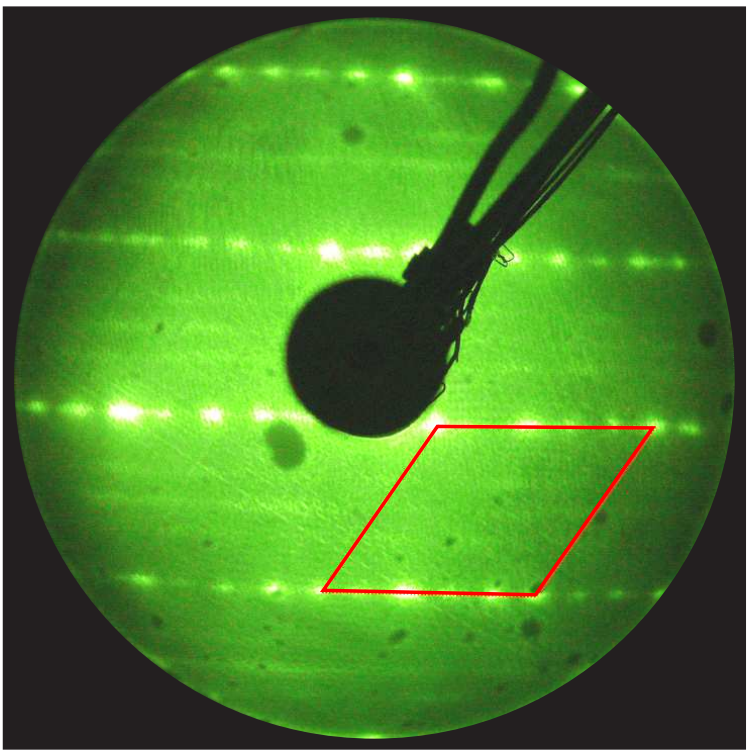

FIG. 2. (Color online) LEED image of Si(553)-Au with faint half- and third-order horizontal streaks indicating the reconstruction of the gold chains and step-edge atoms, respectively. The (1×1) unit cell of the Si substrate is outlined in red.

in this figure. The streaking is due to the poor correlation between the antiphase domains from one chain to the next.[11,22]

Two-photon photoemission (2PPE) experiments were carried out on these samples using femtosecond laser pulses. Infrared ($h\nu_{\mathrm{IR}} = 1.55\,\mathrm{eV}$, pulse duration $\tau_{\mathrm{IR}} \approx 35\,\mathrm{fs}$) radiation was generated by a Ti:sapphire oscillator running at a repetition rate of 80 MHz and a center wavelength of $\lambda_{\mathrm{IR}} = 800\,\mathrm{nm}$. 30% of the IR laser output was sent to the sample via a delay stage. The remaining 70% were fed into a frequency-tripler to generate ultraviolet pulses ($h\nu_{\mathrm{UV}} = 4.65\,\mathrm{eV}$, $\tau_{\mathrm{UV}} \approx 55\,\mathrm{fs}$). For 1PPE experiments the fourth harmonic generated as sum frequency of the IR and UV provided a polarized source of 6.2 eV photons.

The polarizations of the IR and UV beams were rotated independently such that the electric field vector was aligned either perpendicular (s) or parallel (p) to the plane of incidence defined by the direction of the incoming laser pulses and the surface normal. The polarization of the fourth harmonic could also be switched between s and p. Figure 1 depicts the experimental geometry. The angle between incident laser beams and electron analyzer

is fixed at 80°. In normal emission the beams are incident on the sample at a glancing angle of 10°. In this geometry the component of the electric field parallel to the surface may be neglected for p-polarized light. Using optical dipole-selection rules the parity of the electronic states at normal emission, which is even or odd with respect to the $(1\bar{1}0)$ mirror plane orthogonal to the step edges, is evaluated.

Experiments were carried out with this mirror plane oriented parallel or perpendicular to the plane of incidence by *in situ* azimuthal rotation of the sample. The latter orientation corresponds to the $[1\bar{1}0]$ direction denoted $\overline{\Gamma\mathrm{K}}$ in reciprocal space. For the other sample orientation, with the incident light parallel to the mirror plane, strict dipole selection rules for odd and even states apply. However, the opposite $\overline{\Gamma\mathrm{M}}$ and $\overline{\Gamma\mathrm{M}'}$ directions, $[\bar{3}\,\bar{3}\,10]$ and $[3\,3\,\overline{10}]$ respectively, are not equivalent as the $(3\,3\,\overline{10})$ plane is not a mirror plane. This situation applies to all fcc-based (111) surfaces like Si(111).[23] For the $\overline{\Gamma\mathrm{K}}$ direction the $(1\bar{1}0)$ mirror plane ensures a symmetric dispersion.

Photoelectron spectra were recorded using an Omicron EA 125 HR spectrometer with seven Channeltron detectors at an angle and energy resolution of 1.6° and 34 meV, respectively. Data shown were obtained for sample temperature of 90 K; additional data taken at room temperature showed similar results with increased linewidth and lower intensity.

III. RESULTS

A. Energy reference

Photoelectron spectra measure the kinetic energy of the emitted electrons relative to the electrodes of the analyzer. In the single- and two-photon photoemission spectra presented here the kinetic energies range from 0 to 1.2 eV. For metallic surfaces, such as Si(553)-Au, the upper cutoff of the spectra at the Fermi level E_F is a convenient reference level. For bulk silicon the valence band maximum would be the appropriate energy reference, but here it is masked by surface states and band bending. Hence we choose E_F as reference level. This also facilitates the comparison with theory.

In addition, a photovoltage arises at low temperature and high illumination intensities due to a reduction of the band bending at the surface.[24] The photovoltage shifts the whole spectrum by an amount which increases with the laser intensity and saturates when the

bands are completely flat.[25]

Another possible energy reference is the low-energy cutoff of the spectrum which corresponds to the vacuum energy of the sample, provided the work function of the analyzer is lower than that of the sample (which is fulfilled here). However, the work function changes with the quality of the sample preparation. The low-energy cutoff is thus a less reliable reference than the Fermi level.

In order to determine the work function of the sample, the low-energy cutoff is measured for different laser intensities. If a reduction of the laser intensity does not show any further shift of the spectrum, the photovoltage is assumed to be zero and the work function of the sample can be obtained from the known work function of the analyzer. If an increase of the laser intensity does not lead to any further shift of the spectrum, the saturated photovoltage corresponds to flat band conditions of the valence band maximum (VBM) and conduction band minimum (CBM). From the known dopant concentration of the silicon substrate the position of the bulk VBM relative to E_{F} can be calculated. By adding the work function (the distance between E_{F} and the vacuum level), the ionization energy (the distance between VBM and the vacuum level) is obtained. For Si(553)-Au a work function of 4.95 ± 0.03 eV is found, together with an ionization energy of 5.05 ± 0.03 eV.

B. Photoemission spectra

Figure 3 presents 1PPE spectra of Si(553)-Au obtained with the fourth harmonic of 6.2-eV photon energy in normal emission. Top and bottom show data obtained with p- and s-polarization, respectively. Dashed lines are for incident light in the mirror plane (perpendicular to chains and step edges) and solid lines for light perpendicular to the mirror plane. The spectra show two pronounced peaks B at 0.45 eV kinetic energy and D at 0.8 eV. The spectra are normalized to the same height at the low-energy cutoff. Slight variations in the peak positions for different polarizations and orientations might be attributed to background contributions or variation of the sample normal upon rotation. However, the existence of different transitions cannot be excluded.

Peak B corresponds to an occupied initial state 0.79 eV below E_{F}. The polarization dependence indicates an even state with respect to the mirror plane. Perpendicular to the mirror plane the selection rules cannot be applied strictly. The observation of peak B for

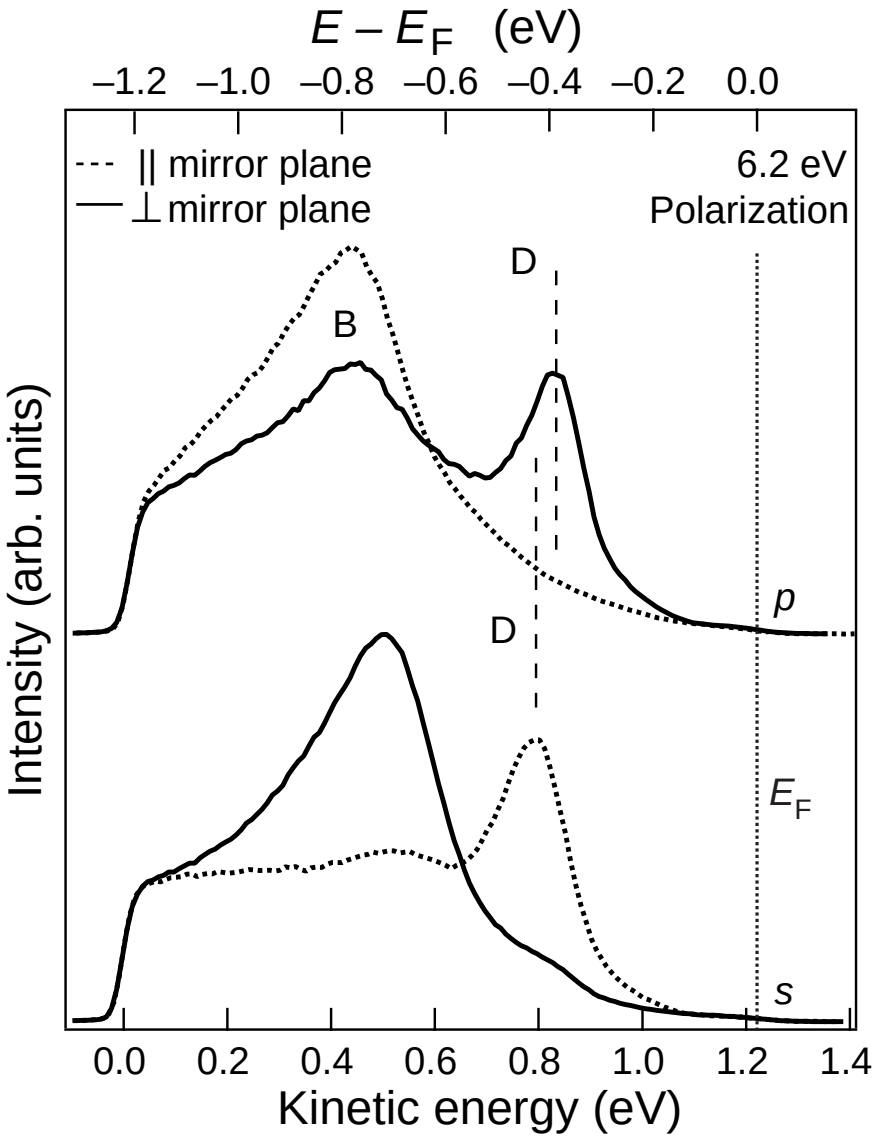

FIG. 3. Polarization-dependent 1PPE spectra recorded with 6.2-eV photons in normal emission for the chains oriented horizontally (solid curves) and vertically (dashed curves). The peaks B (D) represent occupied states that are even (odd) with respect to the mirror plane (cf. Fig. 1).

s- and p-polarized light in that geometry is compatible with an orbital perpendicular to the step edges and significant contribution along the surface normal.

Peak D at 0.45 eV below E_{F} shows the opposite behavior upon sample rotation compared to peak B for s-polarized light. In addition, the peak is not observed for p-polarization in the mirror plane. This proves that peak D corresponds to an initial state of odd symmetry with respect to the mirror plane, e. g. a p_y orbital oriented along the step edges. The orbitals comprising the surface bands in the relevant energy range all have even symmetry (s or p_z).

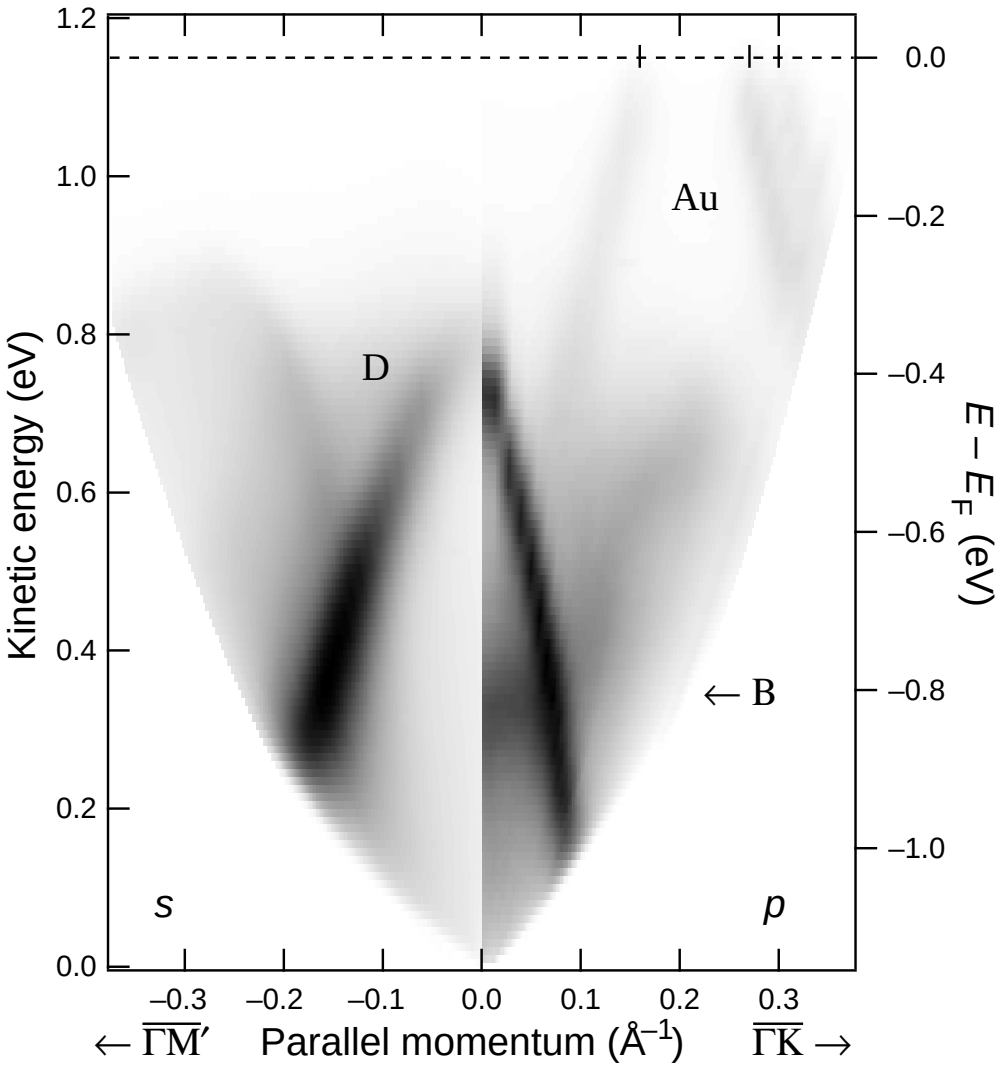

FIG. 4. Photoemission intensity maps ($h\nu = 6.2$ eV) for azimuthal orientations and polarizations showing the downward-dispersing peak D (cf. Fig. 3). In the $\overline{\Gamma K}$ direction the bands assigned to the Au chains with marked Fermi-level crossings can be seen.

However, states of odd symmetry can also be formed from the antisymmetric coupling of base orbitals of even symmetry due to the reconstruction of the Si(553)-Au surface along the step edges. This concept can also explain the observation of states of odd symmetry on the Si(557)-Au surface, which had not been understood before.[20] The odd symmetry of peak D could also be explained by bulk transitions from initial states near the VBM where the heavy-hole band splits into states with even and odd symmetry with repsect to the mirror plane.

Additional information about the character of the observed states can be obtained from

spectra for different emission angles. Angle-resolved data were taken by rotating the sample around the vertical axis in Fig. 1. Depending on the sample orientation, the dispersion perpendicular or parallel to the step edges in the $\overline{\Gamma M}$ or $\overline{\Gamma K}$ direction in the surface Brillouin zone is sampled. Figure 4 shows photoemission intensity excited by 6.2-eV photons in a false color plot as a function of energy relative to E_F and parallel momentum. A peculiar feature of photoemission spectra at such low kinetic energies is the parabolic dependence of the low-energy cutoff on the parallel momentum $k_\parallel$, given by $E_{\mathrm{cutoff}} = \hbar^2 k_\parallel^2 / 2m_e$.[26,27] The polarization was chosen for the two azimuthal orientations such that peak D is observed at normal emission (cf. Fig. 3). Peak D disperses downward with an effective mass of $-0.06\ m_e$ perpendicular to the mirror plane, whereas peak B shows no significant dispersion. The strong negative dispersion of peak D in both azimuthal directions supports the assignment to a bulk transition near the VBM.

Peak B shows strong dispersion for light incident within the mirror plane (see Fig. 5). At normal emission the dispersion exhibits no maximum, but rather a strong slope. Similar behavior is found for the Si(111)-(7×7) surface.[28,29] By time-reversal symmetry the band structure of initial and final states must be symmetric, $E(k_\parallel) = E(-k_\parallel)$. Photoemission from surface states couples directly to free-electron states in front of the surface which can carry the electron toward the detector. Photoemission from bulk bands proceeds via final states in the bulk. Depending on the group velocity $\partial E(k_\perp)/\partial k_\perp$ the electron can propagate towards the surface and be emitted or it disappears into the bulk.[30] The group velocity might change sign by going from $k_\parallel$ to $-k_\parallel$, explaining why a transition might be observed only in certain directions, in particular for the case when the rotation axis is not in a mirror plane. The pronounced asymmetry observed for peak B along $\overline{\mathrm{M\Gamma M'}}$ proves that this feature is due to a bulk transition.

Two additional weaker features appear in the right half of Fig. 4 near the Fermi energy E_F: an upward-dispersing band crossing E_F around 0.16 Å^{-1} and a downward-dispersing double band crossing E_F at 0.27 Å^{-1} and 0.30 Å^{-1}. The latter fits very well to the spin-orbit-split bands of the gold double chain observed previously with higher photon energies.[2] The opposite dispersion direction identifies the single band as the upper Au-atom related band (cf. Fig. 11) backfolded by the (2×1) reconstruction. At higher photon energies this band is observed without backfolding to the first (2×1) Brillouin zone.[2]

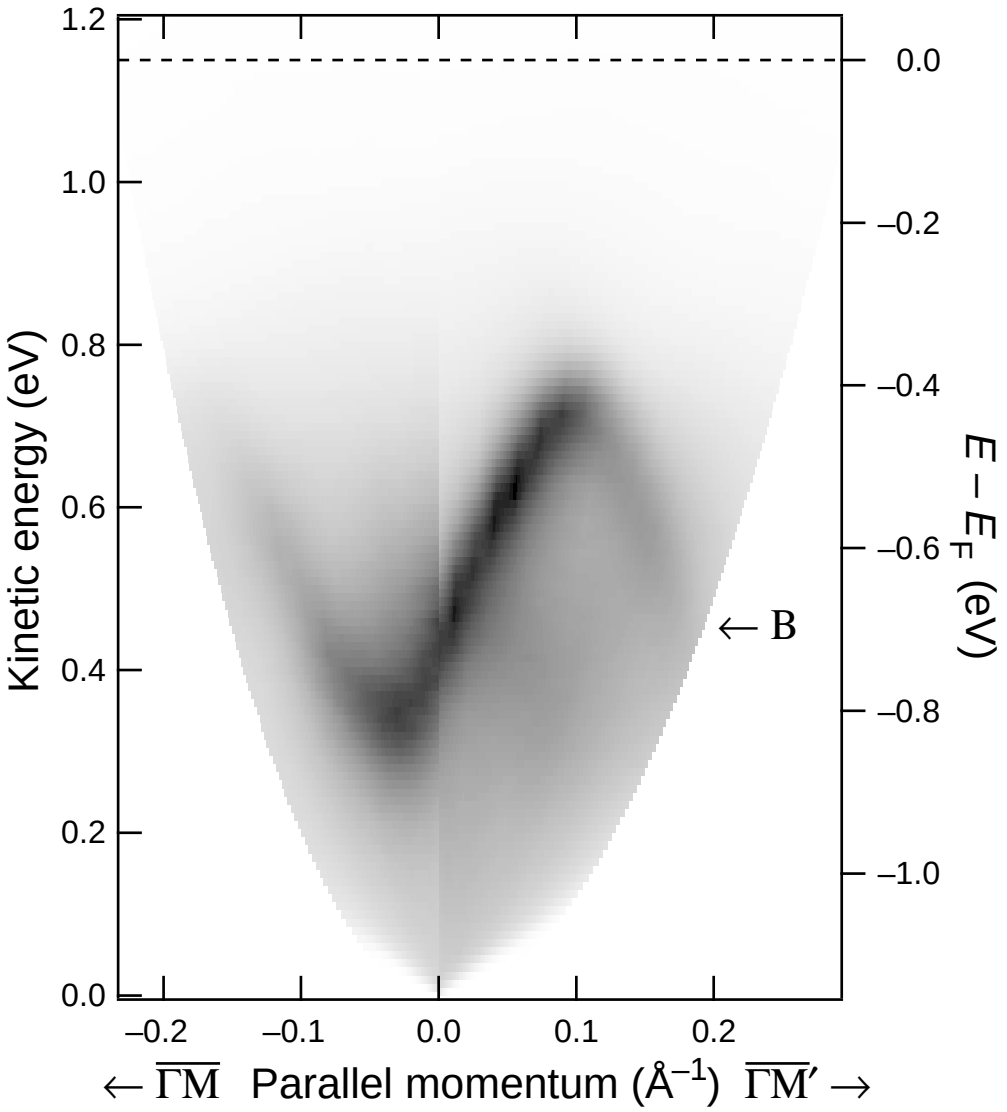

FIG. 5. Photoemission intensity maps in opposite azimuthal directions ($\overline{\Gamma\mathrm{M}}$ and $\overline{\Gamma\mathrm{M}'}$) obtained with p-polarized 6.2 eV photons incident in the mirror plane. The lack of mirror symmetry shows that peak B represents a bulk transition.

C. Two-photon photoemission

The absorption of two photons in 2PPE may proceed from the same initial states as in regular photoemission. In the present experiments the sum of the photon energies in 2PPE, $1h\nu$+$3h\nu$, is equal to the $4h\nu$ used to obtain the 1PPE results presented in the preceding section. Therefore the corresponding peaks assigned to occupied initial states in 2PPE should appear at the same kinetic energies.

In 2PPE spectra additional peaks can arise from intermediate states. These states may be populated and probed by IR or UV photons and may be characterized according to the excitation sequence as $3h\nu$-$1h\nu$ or $1h\nu$-$3h\nu$ processes (see left and right sketches in Fig. 1). The different possibilities may be distinguished by determining the change of the kinetic energy with photon energy $\alpha = d\,E_{\rm kin}/d\,h\nu$. Slope $\alpha = 1$ is found for a $3h\nu$-$1h\nu$ excitation sequence, $\alpha = 3$ for $1h\nu$-$3h\nu$, and $\alpha = 4$ for simultaneous absorption of two photons from an initial state. For $1h\nu$-$1h\nu$ excitation the total photon energy is below the work function and $3h\nu$-$3h\nu$ processes could not be observed lacking sufficient UV intensity.

In the present experimental setup the photon energy $h\nu$ can be varied only in a limited range from 1.51 to 1.58 eV. Therefore the determination of slopes is not very accurate. The assignment of the transitions is corroborated by the polarization dependence of the involved states and by time-resolved data as a function of pump-probe delay.

1. Initial states

Figure 6 depicts spectra obtained for all four possible polarization combinations of the IR and UV laser pulses. Dashed (solid) lines are for the mirror plane oriented parallel (perpendicular) to the plane of incidence. The main peaks observed are labeled A, B and C. In most spectra peak B is observed at 0.45 eV kinetic energy and is readily assigned to the peak B found in Fig. 3. It is suppressed only for *s*-polarized UV photons at light incidence in the mirror plane, where strict dipole selection rules apply. This indicates that the two-photon excitation process involves some intermediate state which is ionized by *p*-polarized UV light. As the transition is observed for *s*- and *p*-polarized IR light, the excitation sequence is $1h\nu$-$3h\nu$ involving an intermediate state of even symmetry populated from even or odd initial states. Peak B in Fig. 3 was assigned to an even state. However, the spectrum for *s*-polarized light in the mirror plane shows a small peak in Fig. 3 and the corresponding peak in the IR-*s* / UV-*p* spectrum of Fig. 6 is also relatively small. Peak B is found in all spectra taken with incident light perpendicular to the mirror plane in single- and two-photon photoemission. That observation provides no further information on the character of initial or intermediate states. The identification of an intermediate state contributing to peak B is at conflict with the assignment as bulk transition from Fig. 3. The intermediate state would also be in the band gap. We conclude that the 2PPE peak B might contain some

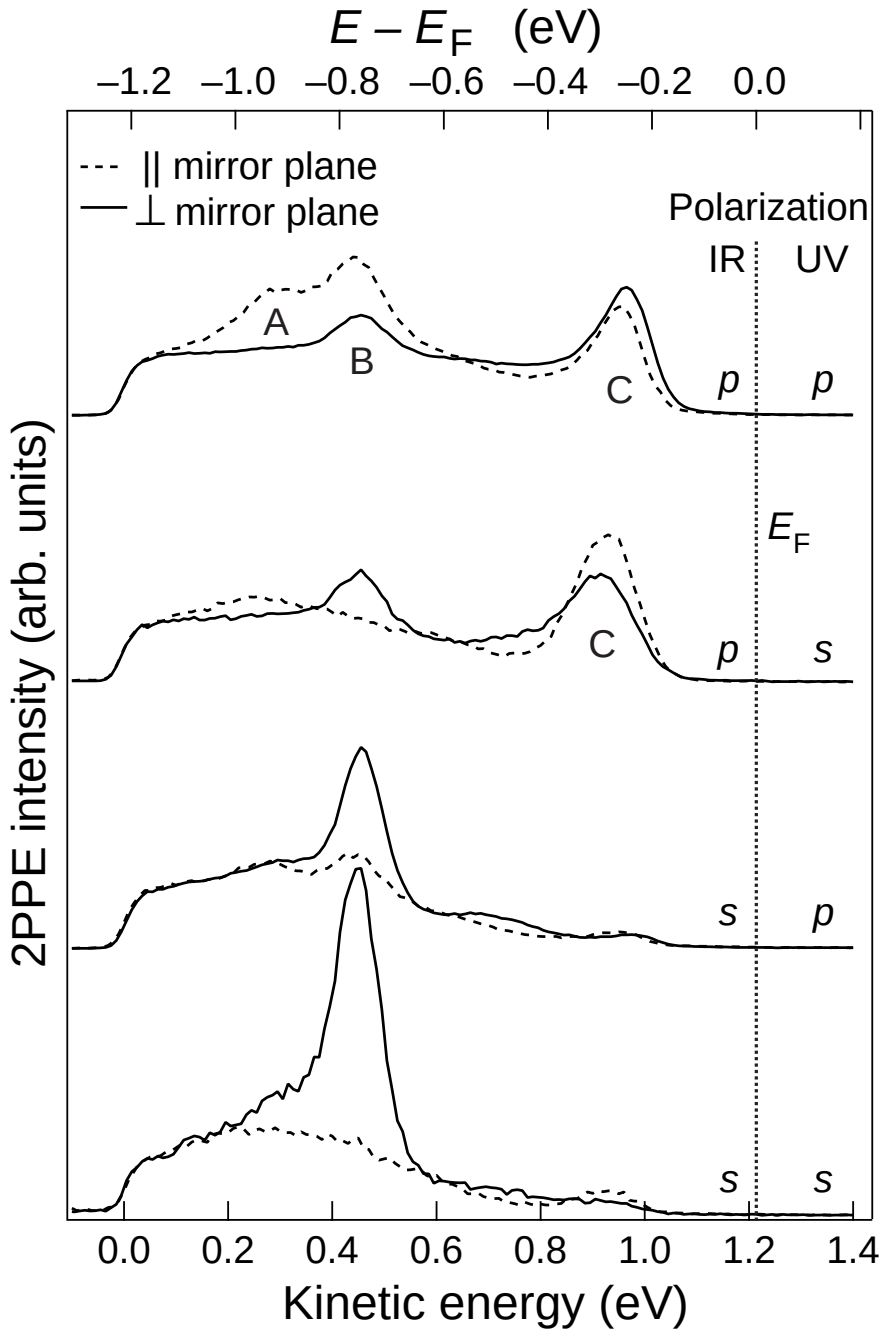

FIG. 6. Two-photon photoemission (2PPE) spectra recorded in normal emission for all polarization combinations of IR and UV photons and for the mirror plane oriented parallel (dashed curves) and perpendicular (solid curves) to the plane of incidence (cf. Fig. 1).

contributions from the initial state observed in Fig. 3, but its main intensity arises from even intermediate states—as will be confirmed below by the dispersion and time-resolved data.

Peak D was observed in 1PPE at $E_{\mathrm{kin}} = 0.8$ eV. None of the 2PPE spectra show a

clear peak at this energy. This suggests that there is no intermediate states for 2PPE transitions available which have sufficient overlap with the initial state or sufficient lifetime to be observed.

At this point we would like to note that neither peak B or D were observed in 2PPE using $2h\nu + 2h\nu$. This finding further supports the existence of an intermediate state for 2PPE transitions B using IR and UV light. For $2h\nu + 2h\nu$ transitions the intermediate state would be in the conduction band providing many possible intermediate states. Possible surface states would have large overlap with bulk states. The resulting short lifetimes would lead to low 2PPE signals.

2. Image-potential state

Peak C is visible in all spectra with a p-polarized IR pulse, which indicates an even intermediate state. The energy of the state lies at $E_{\mathrm{V}} - 0.59$ eV. We assign it to the $n = 1$ image-potential resonance analogous to peak C on the Si(557)-Au surface.[20] Its energy can be calculated with the Rydberg-like formula for image-potential states by taking the dielectric constant of silicon, $\epsilon_r \approx 11.7$, into account.[31,32]

Time-resolved measurements (not shown, for spectra at different time delays see Fig. 8) show a lifetime of 15 fs for peak C pumped by UV ($3h\nu$) and probed by IR ($1h\nu$) pulses, supporting the assignment to an image-potential resonance. A similar lifetime < 10 fs was found on Si(557)-Au.[20] The relatively short lifetimes are in agreement with the location of the states in the conduction-band continuum of the silicon substrate.

Photon-energy-dependent measurements of the energy of peak C indicate a slope $\alpha \approx 3$ for both polarization combinations for which it is observed. This would imply an IR-pump UV-probe process in contrast to the assignment of an image-potential state and the evidence from time-resolved measurements. Due to the limited photon-energy range available, a slope $\alpha \approx 3$ could be explained by overlapping contributions from initial states ($\alpha = 4$) and UV-pumped intermediate states ($\alpha = 1$).[32,33]

Peak C shows measurable dispersion along and perpendicular to the gold chains for both pulses p-polarized as shown in Fig. 7. The effective masses are $m^*_{\parallel \mathrm{C}} = -0.13\, m_e$ along and $m^*_{\perp \mathrm{C}} = -0.14\, m_e$ perpendicular to the chains. Similar values were found for the image-potential resonance on the Si(557)-Au surface.[20] The remarkable strong negative

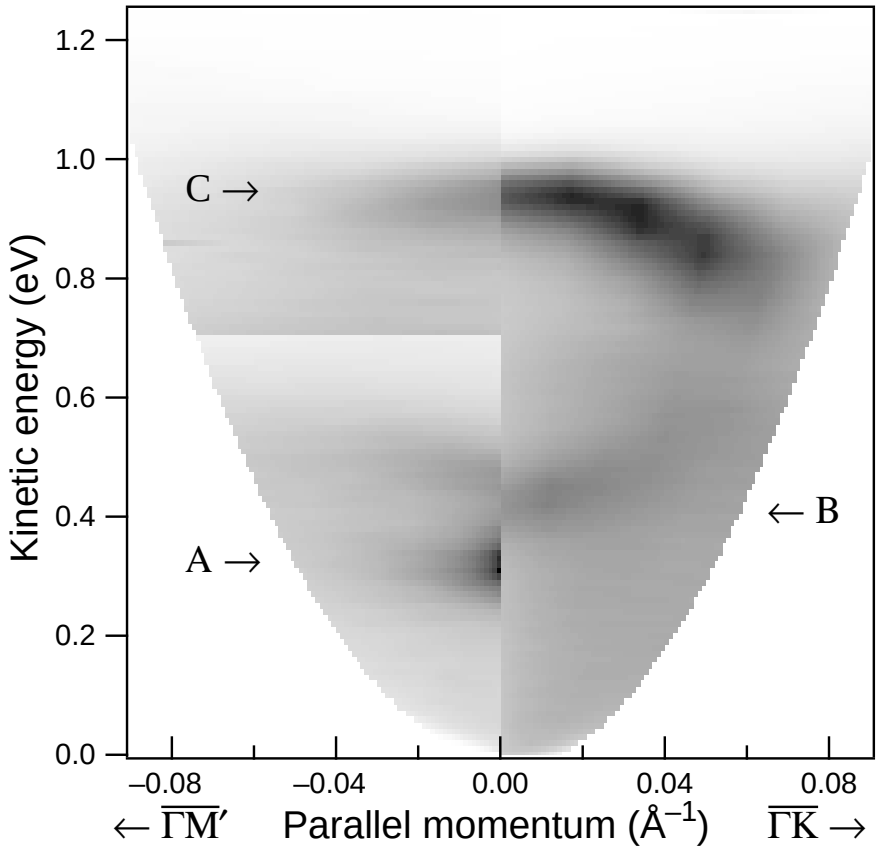

FIG. 7. Dispersion of the image-potential resonance C parallel and perpendicular to the mirror plane. Data were taken with a time delay of 50 fs between the p-polarized UV-pump and IR-probe pulses to enhance the relative intensity of the image-potential resonance. The intensity above 0.7 eV along $\overline{\Gamma M'}$ is enhanced to show the image-potential resonance more clearly.

dispersion of this state might be dominated by an initial state of even symmetry 0.23 eV below the bulk valence-band maximum (VBM) with an effective mass comparable to the light-hole band near the VBM of silicon, which is characterized by an effective mass of $m^*_{\mathrm{lh}} = -0.16\, m_e$.[34] For an image-potential resonance an upward dispersion characterized by the free-electron mass would be expected.[31] This supports the finding from the photon-energy dependence that initial states significantly contribute to peak C. The initial state may dominate the dispersion as observed for the image-potential resonance on the clean Si(100) $c(4 \times 2)$ surface.[32]

For s-polarized UV pulses peak C is found at an energy 0.05 eV lower than for p-polarization. Also the the dispersion becomes weaker with $m^*_{\parallel \mathrm{C}} = -0.28\, m_e$ along the step edges. Perpendicular to the steps in the mirror plane the dispersion is asymmetric

similar to peak B in Fig. 5. This indicates the involvement of bulk bands in this transition. Dipole selection rules demand an initial state of odd parity relative to mirror plane. The doubly-degenerate heavy-hole band of Si splits into odd and even bands in the mirror plane and is characterized by an effective mass of $-0.49\,m_e$ near the VBM.[34]

There is strong evidence for an assignment of peak C to an image-potential resonance from energy, polarization, and lifetime considerations. However, the observed photon-energy and polarization dependence as well as the dispersion indicate significant contributions from initial states near the VBM. At higher photon energies than available in this work this assignment could be confirmed by the observation of the correct slope and dispersion or the second image-potential state.[32,33]

3. Intermediate state

The last feature to be discussed in the two-photon photoemission spectra of Fig. 6 is peak A around 0.3 eV kinetic energy. It is clearly observed only for p-polarized UV light incident in the mirror plane and shows no dispersion (see Fig. 7). The polarization behavior suggests an IR-pump UV-probe process from a state of even symmetry in the mirror plane oriented perpendicular to the step edges. Because it is not clearly observed for the rotated sample orientation, the orbital seems to be oriented more parallel to the surface than perpendicular.

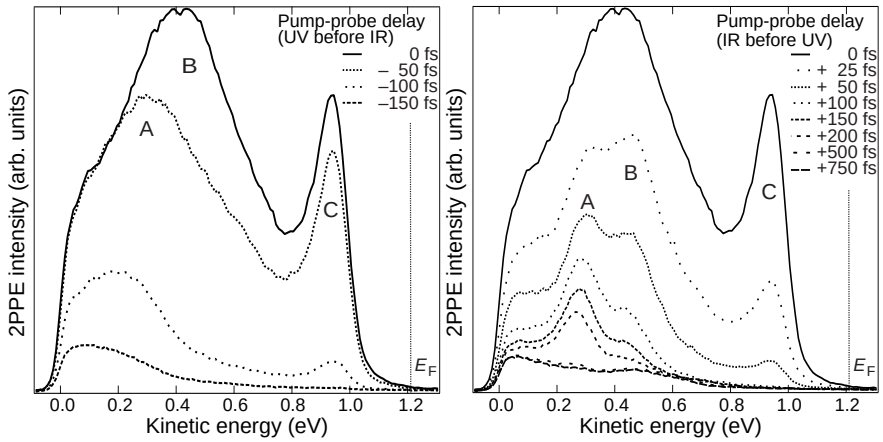

FIG. 8. Photoemission spectra in normal emission for negative (left panel: UV before IR) and positive (right panel: IR before UV) time delays and the mirror plane oriented perpendicular to the plane of incidence (see Fig. 1). All spectra are recorded for both pulses p-polarized.

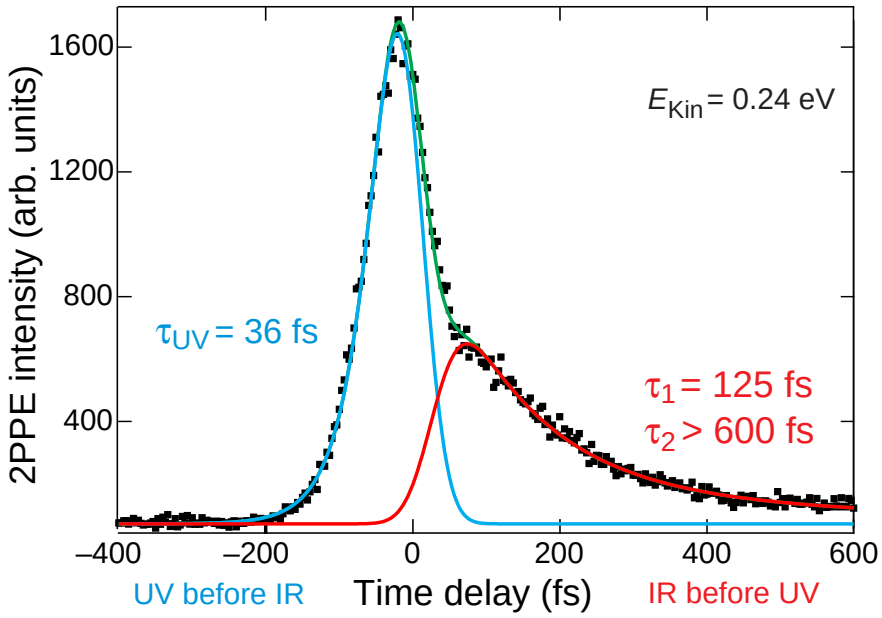

FIG. 9. (Color online) Time-resolved 2PPE intensity of peak A for both pulses being p-polarized. The spectrum shows intensity for negative (UV before IR) and positive (IR before UV) time delays which indicates an UV-pump IR-probe and an IR-probe and UV-pump process, respectively. For positive time delays the decay consists of two decay constants of 125 fs and > 600 fs.

A quantitative analysis of orbital orientation would require more extensive polarization-dependent measurements.[35]

The IR-pump UV-probe process is corroborated by the spectra taken for different time delays Δt presented in Fig. 8. Peak A gains in relative intensity compared to other peaks with increasing positive time delay. Peak C disappears for time delays $|\Delta t| > 150$ fs in agreement with the rather short lifetime of 15 fs mentioned before. Peak B persists for positive time delays up to +500 fs in agreement with the existence of an intermediate state for a $1h\nu$-$3h\nu$ transition.

For a quantitative determination of the lifetime of peak A the intensity as a function of time delay is shown in Fig. 9. The decay can be fitted by two decay times of 125 and > 600 fs. The larger value indicates a delayed filling presumably from electrons excited in the bulk and diffusing towards the surface.[36] The energy of the intermediate state is 0.62 eV above E_F, which is close to the center of the Si bulk band gap. The lack of dispersion indicates a localized state. For these reasons relatively long lifetimes of 125 fs are no surprise. At the same time the localized state in the band gap might serve as an efficient trap for electrons

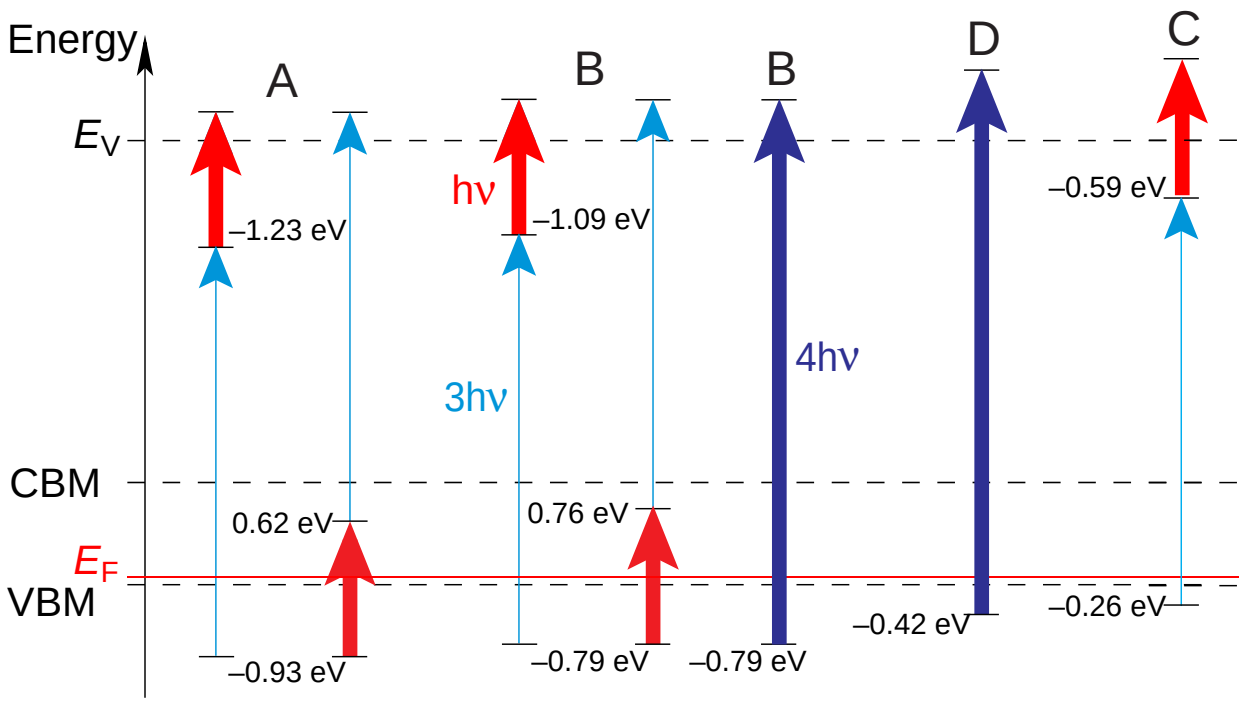

FIG. 10. (Color online) Energy diagram of the observed 2PPE transitions at normal emission. The energies of the intermediate states are referenced to the vacuum level for $3h\nu$-$1h\nu$ processes and to the Fermi energy for $1h\nu$-$3h\nu$ processes.

diffusing in the conduction band towards the surface.

IV. DISCUSSION

The initial-state energies E_i and intermediate-state energies E_m relative to E_F or E_V observed in normal emission (cf. Figs. 3 and 6) are collected in Table I and the transitions are plotted in Fig. 10. For single-photon photoemission no intermediate state energy is given and the photon energy dependence has not been measured. The effective masses depend on the sample orientation. The last two columns in Table I give the polarization combinations where the peaks are observed clearly.

The occurrence of the image-potential resonance C is consistent with the 2PPE results for Si(557)-Au.[20] Very similar observations were made on the clean Si(100) $c(4\times2)$ surface.[32,33] This proves that screening of an external electron leads to image-potential states also on semiconductor substrates. The different energies and effective masses depending on the polarization of the UV photon prove a strong influence of the initial band structure. This

TABLE I. Initial state energies E_i, intermediate state energies E_m, effective masses m^* and polarization combinations (IR/UV for 2PPE) of the observed states for both sample orientations (parallel and perpendicular to the mirror plane). The parameter α is the change of the kinetic energy with photon energy.

Peak	Method	E_i (eV)	E_m (eV)	α	$m^*_\parallel(m_e)$	$m^*_\perp(m_e)$	pol.$_\parallel$	pol.$_\perp$
A	2PPE	$E_\mathrm{F}-0.93$	$E_\mathrm{F}+0.62$	2	∞	∞	*pp,sp*	—
B	2PPE	$E_\mathrm{F}-0.79$	$E_\mathrm{F}+0.76$	2	∞	∞	*pp,sp*	*pp,ps,sp,ss*
B	1PPE	$E_\mathrm{F}-0.79$	—	–	asym.	∞	*p*	*p,s*
D	1PPE	$E_\mathrm{F}-0.42$	—	–	-0.34	-0.06	*s*	*p*
C	2PPE	$E_\mathrm{F}-0.31$	$E_\mathrm{V}-0.63$	3	asym.	-0.28	*ps*	*ps*
C	2PPE	$E_\mathrm{F}-0.26$	$E_\mathrm{V}-0.59$	3	-0.14	-0.13	*pp*	*pp*

explains also the slope $\alpha = 3$ deviating from the expected value of $\alpha = 1$.

The slopes $\alpha = 2$ for 2PPE transitions A and B are not compatible with the expected values of 3 and 4 for intermediate and initial states, respectively. The time-resolved data in Fig. 9 show that peak A has a significant contribution from $3h\nu - 1h\nu$ excitations which would give a slope of 1. The overlap of these two contributions might yield a slope different from the expectation for single transitions. To resolve this issue a larger variation of the photon energy than available in the present setup would be necessary as already discussed for the image-potential resonance.

The bulk transition B can also be found in similar 1PPE measurements on the clean Si(111)(7×7) surface[28] and on the Si(557)-Au[21] surface. The strong polarization-dependent behavior is in good agreement with bulk band structure calculations.[28] The observation of peak B at the same energy in 2PPE as in 1PPE suggests that the same initial state is involved. However, for the 2PPE transition no intermediate bulk band would be available. Also the dispersion is very weak in contrast to the results shown in Fig. 5. As discussed in Section III C 1 the 2PPE transition B seems to be strongly influenced by an intermediate state 0.76 eV above E_F. The time-resolved data in Fig. 9 show a behavior similar to peak A with a lifetime of 30 ± 10 fs. Also the dispersion is quite similar to that of peak A for all four polarization combinations measured. The band structure calculations presented in the following section present a convincing interpretation of peak A, but offer no additional

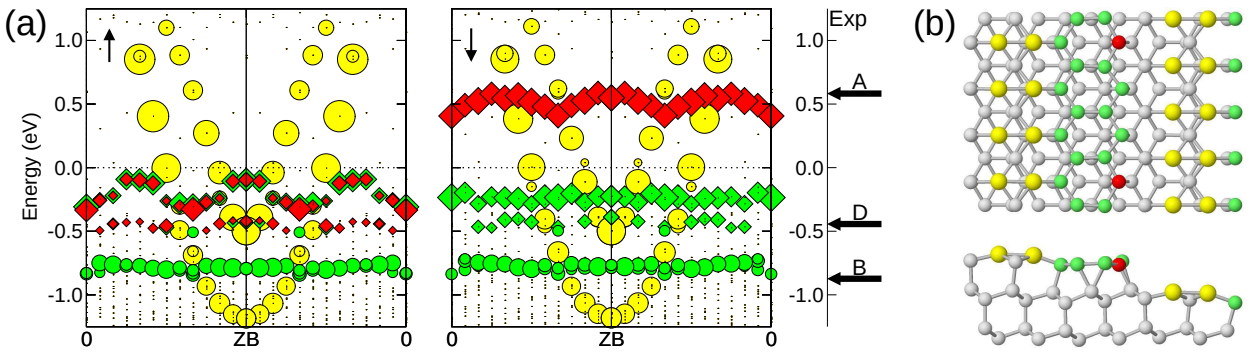

FIG. 11. (Color online) (a) Comparison between theoretical band structure of Si(553)-Au and three states detected experimentally by 2PPE. Colored symbols correspond to the colored atoms in the structural model shown in panel (b). Yellow circles are bonding (lower) and anti-bonding (upper) states from the Au chains, red diamonds are exchange-split states from spin-polarized Si atoms at the step edge, green diamonds are states from non-polarized Si step-edge atoms, and green circles are states from non-polarized Si atoms on the opposite side of the honeycomb chain. The zone boundary (ZB) is that of the 1×1 unit cell. Because the actual cell is 1×3 cell (we used a ferromagnetic array of polarized Si atoms rather than the full 1×6 antiferromagnetic array of Ref. 7) we unfolded the 1×3 Au bands into the 1×1 cell for easier visualization.

intermediate state slightly above A near $\overline{\Gamma}$. A consistent interpretation of the experimental data can be obtained by assigning peak B to an initial state which is observed by an off-resonant 2PPE transition[37] involving the intermediate state A.

In comparison to the 2PPE study of Si(557)-Au[20] the closest similarity is found for the image-potential resonance C. Peak A shows somewhat similar behavior regarding the long lifetime of intermediate states close to the center of the band gap. The peak labeled B in the Si(557)-Au study shows upward dispersion and is located close to the conduction minimum.[20] There is no comparable state found on Si(553)-Au. For the peaks B and D observed in 1PPE similar transitions are found also on Si(557)-Au.[21] This supports an assignment to the same bulk transitions as observed on the clean Si(111)-(7 × 7) surface.[28] The 2PPE peak B as well as peak A involve intermediate states in the bulk band gap. These states must be characteristic features of the electronic and geometric structure of the Si(553)-Au surface.

V. THEORETICAL BAND STRUCTURE

To help identify the origin of the observed peaks, we performed first-principles calculations of the electronic structure of Si(557)-Au using the structural model proposed in Ref. 7. The calculations were performed in a slab geometry with six or more layers of Si plus the reconstructed top surface layer and a vacuum region of at least 10 Å. All atomic positions were relaxed, except the bottom Si layer and its passivating hydrogen layer, until the largest force component on every atom was below 0.02 eV/Å. Total energies and forces were calculated within the Perdew-Burke-Ernzerhof (PBE) generalized-gradient approximation[38] to DFT using projector-augmented-wave (PAW) potentials, as implemented in VASP.[39,40] The plane-wave cutoff for all calculations was 250 eV.

It is important to realize that the electronic states arising from Si surface orbitals are here quite narrow—less than 0.5 eV—and therefore may be subject to electron correlation effects not accurately described by PBE. For this reason we used the screened hybrid functional of Heyd, Scuseria, and Ernzerhof (HSE)[41,42] to calculate the electronic band structure. The HSE functional replaces a fraction of the PBE exchange potential by the exact Hartree-Fock exchange potential and generally leads to a more accurate description of the electronic properties of many materials. In this work we are mainly interested in the states related to Si surface dangling bonds. For this reason we used a mixing fraction, $a = 0.11$, previously shown to give an accurate description of the dangling bond in bulk Si.[43]

The resulting spin-polarized HSE band structure is shown in Fig. 11. The main features are very similar to those obtained using standard PBE and were already discussed in Ref. 7. One important difference arises from the HSE hybrid functional: the unoccupied spin-split Si step-edge band is shifted upward, to 0.5 eV, significantly higher than the PBE value of 0.3 eV. This shift indicates the important role of electron correlation within this spin-polarized Si dangling-bond state.

Figure 11 also shows a comparison between the theoretical band structure and the peaks detected by 2PPE. The red unoccupied spin-down band matches well the observed peak A. Peak D could be assigned to the green step-edge band and/or the red occupied spin-up band, which are closely superimposed. The observed odd symmetry along the step edges may correspond to the antibonding combination of the orbitals on two neighboring non-polarized step-edge atoms. However, the observed dispersion is at variance with the calculated band

structure. Peak B matches closely the band of the non-polarized step-edge atoms.

VI. CONCLUSIONS

Stepped surfaces with large unit cells, such as Si(553)-Au, contain many different structural elements and pose a challenge for theoretical calculations, structural analyses and spectroscopies. The recent prediction of spin-polarized step-edge atoms adds a new element. Using one- and two-photon photoemission we are able to confirm spectroscopically the spin-polarized band structure of Si(553)-Au by detecting the split-off minority spin state. It lies in the band gap of silicon, well-separated from bulk states and other surface states. Complete control of the polarization via laser sources facilitates the determination of the parity and thereby aids with the assignment of specific states. It also yields surprises such as anti-symmetric states constructed from symmetric basis orbitals by backfolding. Bulk transitions lead to apparently asymmetric bands. They also can alter the measured dispersion of surface bands, such as image-potential states. The present work shows that two-photon photoemission can be applied successfully to rather complicated surface structures. Thorough analysis of a complete data set permits a detailed comparison to the results of band structure calculations. An extended range of photon energies could provide additional insight as has been shown for other Si surfaces.[33,44]

ACKNOWLEDGMENTS

Part of this work was supported by the Office of Naval Research. The DFT computations were performed at the DoD Major Shared Resource Centers at AFRL and ERDC. FJH acknowledges support by the NSF under Award No. DMR-0705145.

---

[1] J. N. Crain and F. J. Himpsel, Appl. Phys. A **82**, 431 (2006).

[2] J. N. Crain, J. L. McChesney, F. Zheng, M. C. Gallagher, P. C. Snijders, M. Bissen, C. Gundelach, S. C. Erwin, and F. J. Himpsel, Phys. Rev. B **69**, 125401 (2004).

[3] S. Riikonen and D. Sánchez-Portal, Phys. Rev. B **71**, 235423 (2005).

[4] S. Riikonen and D. Sánchez-Portal, Surf. Sci. **600**, 1201 (2006).

[5] S. Riikonen and D. Sánchez-Portal, Phys. Rev. B **77**, 165418 (2008).

[6] M. Krawiec, Phys. Rev. B **81**, 115436 (2010).

[7] S. C. Erwin and F. J. Himpsel, Nature Commun. **1**, 58 (2010).

[8] J. N. Crain, A. Kirakosian, K. N. Altmann, C. Bromberger, S. C. Erwin, J. L. McChesney, J.-L. Lin, and F. J. Himpsel, Phys. Rev. Lett. **90**, 176805 (2003).

[9] J. R. Ahn, P. G. Kang, K. D. Ryang, and H. W. Yeom, Phys. Rev. Lett. **95**, 196402 (2005).

[10] P. C. Snijders, S. Rogge, and H. H. Weitering, Phys. Rev. Lett. **96**, 076801 (2006).

[11] J. N. Crain, M. D. Stiles, J. A. Stroscio, and D. T. Pierce, Phys. Rev. Lett. **96**, 156801 (2006).

[12] K.-D. Ryang, P. G. Kang, H. W. Yeom, and S. Jeong, Phys. Rev. B **76**, 205325 (2007).

[13] P.-G. Kang, J. S. Shin, and H. W. Yeom, Surf. Sci. **603**, 2588 (2009).

[14] I. Barke, F. Zheng, T. K. Rügheimer, and F. J. Himpsel, Phys. Rev. Lett. **97**, 226405 (2006).

[15] I. Barke, R. Bennewitz, J. N. Crain, S. C. Erwin, A. Kirakosian, J. L. McChesney, and F. J. Himpsel, Solid State Commun. **142**, 617 (2007).

[16] S. K. Ghose, I. K. Robinson, P. A. Bennett, and F. J. Himpsel, Surf. Sci. **581**, 199 (2005).

[17] W. Voegeli, T. Takayama, K. Kubo, M. Abe, Y. Iwasawa, T. Shirasawa, T. Takahashi, K. Akimoto, H. Sugiyama, H. Tajiri, K. Akimoto, H. Sugiyama, H. Tajiri, and O. Sakata, e-J. Surf. Sci. Nanotechnol. **6**, 281 (2008).

[18] T. Takayama, W. Voegeli, T. Shirasawa, K. Kubo, M. Abe, T. Takahashi, K. Akimoto, and H. Sugiyama, e-J. Surf. Sci. Nanotechnol. **7**, 533 (2009).

[19] I. Barke, F. Zheng, S. Bockenhauer, V. v. Oeynhausen, K. H. Meiwes-Broer, S. C. Erwin, and F. J. Himpsel, Phys. Rev. B **79**, 155301 (2009).

[20] T. K. Rügheimer, Th. Fauster, and F. J. Himpsel, Phys. Rev. B **75**, 121401 (2007).

[21] T. K. Rügheimer and Th. Fauster, (2006), unpublished results.

[22] A. Kirakosian, R. Bennewitz, F. J. Himpsel, and L. W. Bruch, Phys. Rev. B **67**, 205412 (2003).

[23] E. W. Plummer and W. Eberhardt, "Angle-resolved photoemission as a tool for the study of surfaces," (John Wiley & Sons, Inc., New York, 1982) pp. 533–656.

[24] W. Mönch, *Semiconductor Surfaces and Interfaces* (Springer Verlag, Berlin, Heidelberg, 2001).

[25] A. Melzer, D. Kampa, J. Wang, and Th. Fauster, Phys. Rev. B **80**, 205424 (2009).

[26] M. Cardona and L. Ley, eds., *Photoemission in Solids I*, Top. Appl. Phys., Vol. 26 (Springer, Berlin, 1978) Chap. 1.

[27] F. Bisio, M. Nývlt, J. Franta, H. Petek, and J. Kirschner, Phys. Rev. Lett. **96**, 087601 (2006).

[28] W. Heckel, K. Biedermann, Th. Fauster, and F. J. Himpsel, (2011), unpublished results.

[29] R. I. G. Uhrberg, G. V. Hansson, U. O. Karlsson, J. M. Nicholls, P. E. S. Persson, S. A. Flodström, R. Engelhardt, and E.-E. Koch, Phys. Rev. B **31**, 3795 (1985).

[30] W. Schattke, E. E. Krasovskii, R. Díez Muiño, and P. M. Echenique, Phys. Rev. B **78**, 155314 (2008).

[31] P. M. Echenique and J. B. Pendry, J. Phys. C **11**, 2065 (1978).

[32] M. Kutschera, M. Weinelt, M. Rohlfing, and Th. Fauster, Appl. Phys. A **88**, 519 (2007).

[33] C. Eickhoff, M. Teichmann, and M. Weinelt, Phys. Rev. Lett. **107**, 176804 (2011).

[34] M. Levinshtein, S. Rumyantsev, and M. Shur, *Handbook Series on Semiconductor Parameters*, Vol. 1 (World Scientific, Singapore, 1996).

[35] M. Wolf, A. Hotzel, E. Knoesel, and D. Velic, Phys. Rev. B **59**, 5926 (1999).

[36] S. Tanaka, T. Ichibayashi, and K. Tanimura, Phys. Rev. B **79**, 155313 (2009).

[37] M. Wolf, E. Knoesel, and T. Hertel, Phys. Rev. B **54**, R5295 (1996).

[38] J. P. Perdew, K. Burke, and M. Ernzerhof, Phys. Rev. Lett. **77**, 3865 (1996).

[39] G. Kresse and J. Hafner, Phys. Rev. B **47**, 558 (1993).

[40] G. Kresse and J. Furthmüller, Phys. Rev. B **54**, 11169 (1996).

[41] J. Heyd, G. E. Scuseria, and M. Ernzerhof, J. Chem. Phys. **118**, 8207 (2003).

[42] J. Heyd, G. E. Scuseria, and M. Ernzerhof, J. Chem. Phys. **124**, 219906 (2006).

[43] P. Broqvist, A. Alkauskas, and A. Pasquarello, Phys. Rev. B **78**, 075203 (2008).

[44] Th. Fauster, S. Tanaka, and K. Tanimura, Phys. Rev. B **84**, 235444 (2011).